Journal of Remote Sensing & GIS

Research Article

Open Access

Evaluation of Automatic Shadow Detection Approaches Using ADS-40 High Radiometric Resolution Aerial Images at High Mountainous Region

Jan-Chang C[1]*, Yi-Ta H[1], Chaur-Tzuhn C[1] and Shou-Tsung W[2]

[1]*Department of Forestry, National Pingtung University of Science and Technology, Pingtung, Taiwan*

[2]*Department of Tourism Management, Shih Chien University, Kaohsiung, Taiwan*

***Corresponding author:** Jan-Chang C, Department of Forestry, National Pingtung University of Science and Technology, No. 1, Shuehfu Road, Neipu, Pingtung, Taiwan, Tel: 88687703202; E-mail: zzzjohn@mail.npust.edu.tw

Abstract

Shadow detection is a very important pre-processing step for remote sensing applications, particularly for high spatial resolution data. This study adopts the high resolution aerial images to investigate the shadow detection issue. Testing three shadow detection methods (Brightness method, Nagao's method, NIR method), and look for a suitable shadow detection method for high radiometric resolution aerial images. We also discuss the differences for each method. The results indicate Brightness method and Nagao's method are significantly better than NIR method. NIR often confuses water bodies with shadows due to the low reflectance of water. The data space we used, Nagao's modified intensity and brightness are better than NIR channel to discriminate shadows from non-shadows, and the two methods are both not easily confused with shadow and water bodies. In our study, we found that most of cases presented shadow in the histogram of first mode, and the first valley detection thresholding is a robust way to detect the shadow threshold of histogram. A good data space and defining the optimum thresholding method will affect histogram thresholding result.

Keywords: Shadow; ADS-40; High radiometric resolution; Mountainous regions

Introduction

Shadow detection is a very important pre-processing step for remote sensing applications, particularly for high spatial resolution data. Regarding shadow detection, the application of invariant color models [1-3], the histogram thresholding method [4-10], 3D modeling processes [11,12], object segmentation methods [2] and hierarchical shadow detection algorithms [13], the above methods have all been shown to produce excellent results.

For the mountain environment, 3D shadow detection are not easily performed, because those techniques require an accurate Digital Surface Model (DSM), and the accuracy of 3D modeling methods is directly limited by the accuracy of the DSM [3]. Therefore, the 2D shadow detection techniques are proposed in mountainous environments.

In previous study, Adeline et al. [3] compare many shadow detection methods for digital aerial images, and the results indicate that histogram thresholding performed the better result. Histogram thresholding is the simplest shadow detection tools but also the most popular in the literature. Histogram thresholding is an ideal method of shadow detection in high resolution satellite images due to the spectral content of the images [7]. The histogram for the Ikonos panchromatic image is clear from the bimodal nature of that there are two predominant features [7].

There are many kinds histogram thresholding method for shadow detection has been published [3-9]. However, those histogram thresholding method depend on the selected data space and thresholding method [3,7].

This study adopts the high radiometric resolution aerial images to investigate the shadow detection issue. Testing different shadow detection methods, and look for a suitable shadow detection method for high radiometric resolution aerial images. We also discuss the differences for each method.

Study Area and Materials

Study area

The research site is located at the Da-Chia stream working cycle, Central Taiwan. The landscape of the research site is characterized as alpine terrain. Its elevation ranges between 743-3,882 m, and shows significant topographical changes. Da-Chia stream working cycle is under the jurisdiction of Dongshi forest district office of forest bureau, total 85 compartments contained. The area is located in upstream of Da-Chia stream and Peikang stream, between Syushan and Central Mountain.

We set 10 image analysis plots (Figure 1), the size of each plot is 1 Km^2, each plot has two period of images, and the detail information was shown in Table 1.
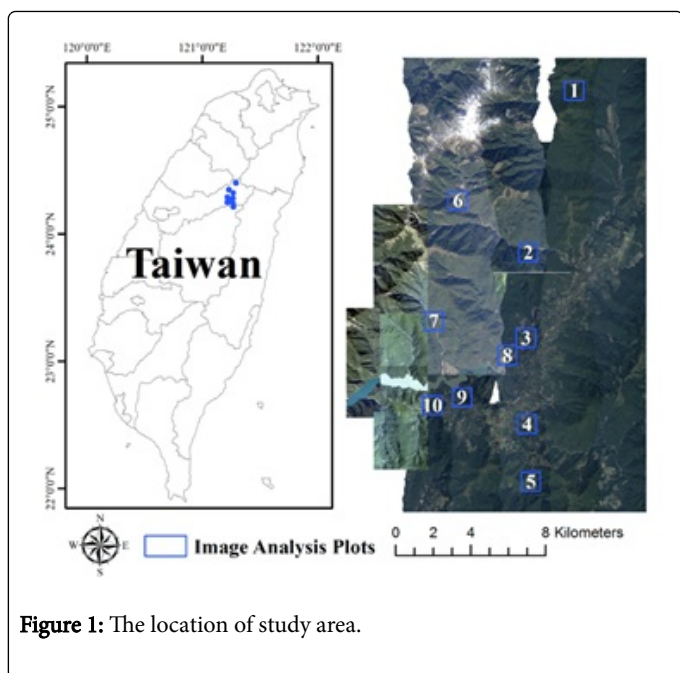
Figure 1: The location of study area.

Plot	Sensor	Date
Plot 1	ADS-40	2008/09/21/10:42
Plot 2	ADS-40	2009/01/02/12:22
Plot 3	ADS-40	2008/09/21/09:58
Plot4	ADS-40	2008/12/27//11:20
Plot5	ADS-40	2008/12/27/11:20
Plot6	ADS-40	2009/01/02/12:05
Plot7	ADS-40	2009/01/02/12:05
Plot8	ADS-40	2008/09/21/09:50
Plot9	ADS-40	2008/09/21/10:05
Plot10	ADS-40	2008/09/21/10:05

Table 1: Data use of 10 image analysis plots.

Digital aerial images

Leica ADS40 are used in this study. The capturing of ADS-40 were conducted by the Aerial Survey Office, Forestry Bureau of Taiwan (Figure 1). Digital Aerial Images were captured between 2007/10/27 and 2009/01/02 (most in 2008/09). The ADS-40 images underwent a series of image processing procedures to produce Level 2 multispectral ortho-image product, in which the Leica Photogrammetry Suite (LPS), Orima, and OrthoVista processing software were used for aerotriangulation and orthorectification procedures, and the Leica Inertial Position and Attitude System (IPAS) and the Waypoint GrafNav/GrafNet software were used for inertial measurement unit and global positioning system (GPS/IMU) processing [13].

The spatial resolution of the ADS-40 ortho-images was 25 cm, providing detailed surface properties. The ADS-40 image comprised four multispectral bands (namely, red (R)=wavelength 610-660 nm; green (G)=wavelength 535-585 nm; blue (B)=wavelength 430-490 nm; and near-infrared (NIR)=wavelength 835-885 nm). In addition, the images presented 14 bit radiometric resolution and excellent signal to noise ratios. The multispectral band data can be recorded up to a 13 bit (digital number (DN) range: 0-8,191) grayscale range, and the panchromatic band can be recorded up to a 14 bit (DN range: 0-16,383) grayscale range [14]. The multispectral band was analyzed in this study. The images were stored in a 16-bit format, but retained their original radiometric resolutions (multispectral band=13 bits).

Methods

Shadow detection is a very important pre-processing step for many remote sensing applications, especially using high spatial resolution remote sensing data. Therefore, this study tested three kinds of shadow detection methods in very high spatial resolution aerial images. We set 10 image analysis plots, and the three shadow detection methods were all performed for each plot.

Optimal thresholding on NIR

The first method, we applied optimal thresholding on NIR (further refer to NIR method). The threshold was determined by using visual selection from the histogram of NIR, and a repeated and exhaustive search for the optimal threshold was performed.

First valley detection thresholding on Nagao's modified intensity

The second method, we applied first valley detection thresholding on Nagao's modified intensity (further refer to Nagao's method). This procedure was using equation (1) [4].

$$I = \frac{1}{6} \times (2RED + GREEN + BLUE + 2NIR)\ (1)$$

I=Nagao's modified intensity; RED=red waveband; GREEN=green waveband; BLUE=blue waveband; and NIR=near-infrared waveband.

The difference between the shadow and non-shadow areas was enhanced by using Nagao's modified intensity image before dividing the image into the respective shadow and non-shadow areas. Because of the location of the shadows in the histograms that mainly occupies the first mode, and the thresholds of shadow areas can be determined by using the first valley detection method [3].

First valley detection thresholding on brightness

The third method, we applied first valley detection thresholding on brightness (further refer to Brightness method). The third method was conducted by using brightness, which was defined as the mean of the four bands (red, green, blue, and NIR), and brightness using equation (2).

$$Bri = \frac{1}{4} \times (RED + GREEN + BLUE + NIR) \qquad (2)$$

Bri=brightness; RED=red waveband; GREEN=green waveband; BLUE=blue waveband; and NIR=near-infrared waveband.

After enhancing the difference between the shadow and non-shadow areas by using brightness, and the threshold of shadow area was also determined by using the first valley detection method.

Accuracy assessment for shadow detection

The accuracy of shadow detection was assessed, and the 200 random points were generated for each plot. The overall accuracy, user's accuracy, producer's accuracy, and Kappa values were employed to determine accuracy. On the other hand, the overall accuracy measures the accuracy of both shadow and non-shadow by treating them equally regardless class sample sizes; for small amount shadow pixels a high accuracy does not necessarily indicate good shadow detection accuracy [3]. F-score, which combines both recall rates (Producer's accuracy) and precision rate (User's accuracy) gives a good balance between under and over detection accuracies [15]. The F-score was also chosen to rank the chosen methods, and F-score using equation (3).

$$F = 2 \times \frac{PA_S \times UA_S}{PA_S + UA_S} \qquad (3)$$

F is the F-score, PAs is the producer's accuracies of shadow, UAs is the user's accuracies of shadow.

To evaluate the differences of the three shadow detection methods, a one-way analysis of variance (one-way ANOVA) was also used to analyze the accuracies variables of the three shadow detection methods, and overall accuracy, Kappa values, and F-score were used as the accuracies variables. The test hypotheses were: H0 (there was no difference in those accuracy variables among the 3 shadow detection methods) and H1 (there were differences in those accuracy variables among the 3 shadow detection methods). The significance level was set to 5%. In order to test the significance of each shadow detection method, Fisher's least significant difference (LSD) test was calculated in a post-hoc analysis. The results are useful in determining which method provides better detection of shadow.

Results and Discussion

Shadow detection accuracy

In this study, we set 10 image analysis plots, and the shadow detection is performing for each plot. Three shadow detection methods (NIR method, Nagao's method, Brightness method) were used in this study.

The grayscale value in the shadow area for three shadow detection methods are calculated during shadow detection, showed lower and presented a darker tone in plot 7 and plot 4 in Figure 2a-2c and Figure 3a-3c. Subsequent to the optimal thresholds for NIR is show in Figure 2g and Figure 3g. First valley detection, the first mode thresholds for Nagao's modified intensity has shown in Figure 2h and Figure 3h. First valley detection, the first mode thresholds for brightness has shown in Figure 2i and Figure 3i. The shadow detection results are consistent with the actual shadow distribution in the images (Figure 2e-2g and Figure 3e-3g). In our study, we find that most of cases present shadow in the histogram of first mode. However, in the plot 4 case, we also notice that two peaks below the optimal thresholds in the histogram of NIR (Figure 2g), and Nagao's modified intensity and brightness has shown bimodal distribution in the histogram (Figure 2h and 2i).
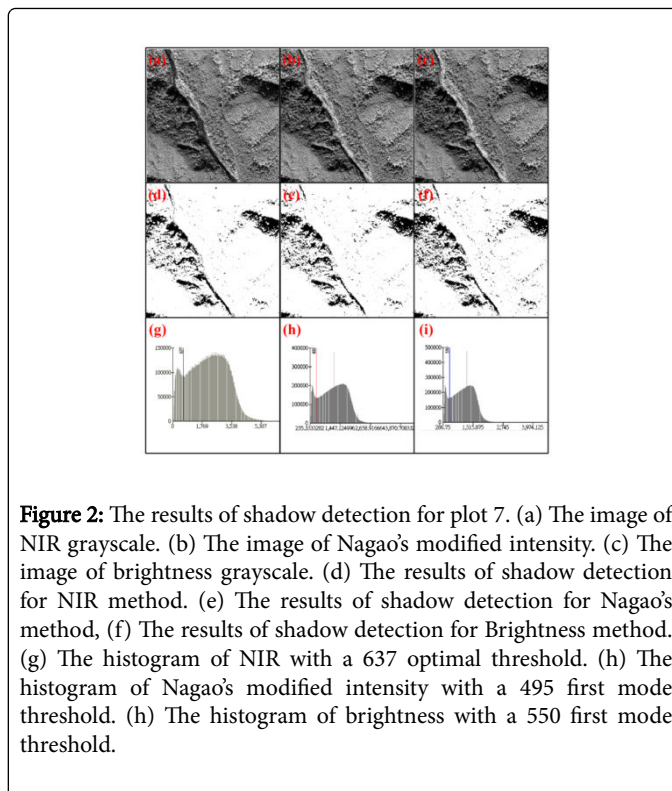
Figure 2: The results of shadow detection for plot 7. (a) The image of NIR grayscale. (b) The image of Nagao's modified intensity. (c) The image of brightness grayscale. (d) The results of shadow detection for NIR method. (e) The results of shadow detection for Nagao's method, (f) The results of shadow detection for Brightness method. (g) The histogram of NIR with a 637 optimal threshold. (h) The histogram of Nagao's modified intensity with a 495 first mode threshold. (h) The histogram of brightness with a 550 first mode threshold.
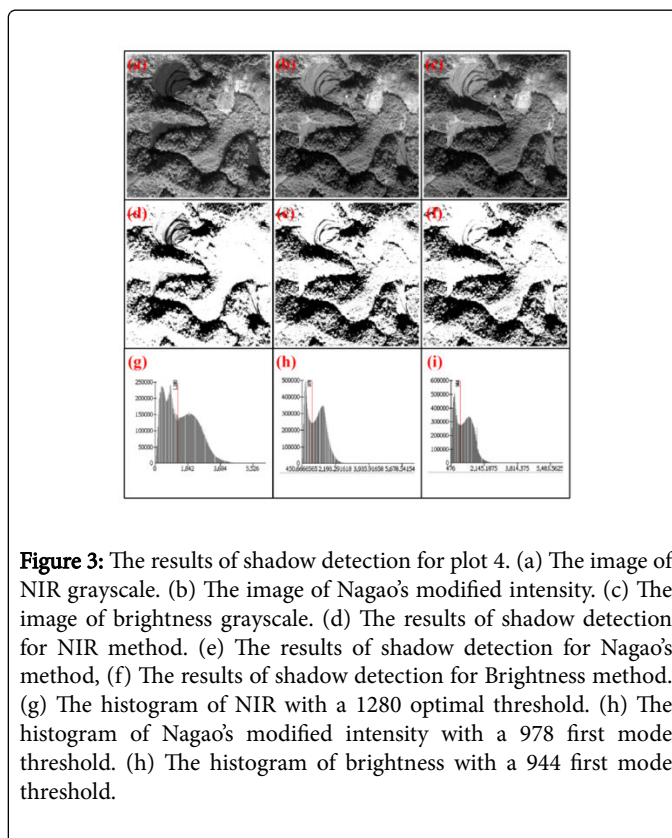
Figure 3: The results of shadow detection for plot 4. (a) The image of NIR grayscale. (b) The image of Nagao's modified intensity. (c) The image of brightness grayscale. (d) The results of shadow detection for NIR method. (e) The results of shadow detection for Nagao's method. (f) The results of shadow detection for Brightness method. (g) The histogram of NIR with a 1280 optimal threshold. (h) The histogram of Nagao's modified intensity with a 978 first mode threshold. (h) The histogram of brightness with a 944 first mode threshold.

With regard to the shadow detection results of all plots, the average overall accuracy of the NIR method is 90.6%, and the average overall kappa value is 0.7552; the average of overall classification accuracy of

Nagao's method is 94.45%, and the overall kappa value is 0.8598; the average overall classification accuracy of Brightness method is 94.75% and the overall kappa value is 0.8640 (Table 2). Brightness method obtained the highest average of overall accuracy result (94.75%), followed by Nagao's method (94.45%) and NIR method (90.60%) performs the lowest accuracy. A comparison of the results from the F-score shows that Brightness method performs the best (F-score average 90.11), followed by Nagao's method (F-score average 89.92), and NIR method (F-score average 82.10) performs the lowest (Table 2). F-score shows the same result as overall accuracy. The accuracy table of 10 plots is show in Appendix Tables 1, 2 and 3. The shadow detection bitmap of 10 plots is also show in Appendix Figures 1 and 2.

Methods	Average overall accuracy (%)	Average Kappa
NIR method	90.60 (3.22)	0.7552 (0.0913)
Nagao's method	94.45 (2.49)	0.8598 (0.0575)
Brightness method	94.75 (2.76)	0.8640 (0.0731)

Table 2: Summary of shadow detection results of 10 image analysis plots.
Note: Mean (standard deviation).

In order to evaluate the differences of the three shadow detection methods, a one-way ANOVA was used to analyze the accuracies variables of the three shadow detection methods. The result indicates that overall accuracy, Kappa, F-score all showed significantly different in the three shadow detection method (Table 3). And we using the LSD test for the three classification methods revealed that the overall accuracy of Nagao's method was significantly better than NIR method; the overall accuracy of Brightness method is also significantly difference with NIR method (Table 3). However, Nagao's method and Brightness method are show no significantly different in overall accuracy. The result of Kappa, F-score using LSD tests for the three classification methods are also showed the same results as the overall accuracy (Table 3).

	F	Sig (<α=0.05*)	NIR method	Nagao's method	Brightness method
Overall accuracy (%)	6.641	0.005*	90.60a	94.45b	94.75b
Kappa	6.704	0.004*	0.755a	0.860 b	0.864 b
F-score	5.546	0.010*	82.099 a	89.923 b	90.114 b

Table 3: Results of one-way ANOVA and LSD test.
In a row followed by the same letter do not significantly differ.

We compare the shadow bitmaps of three shadow detection methods, and we see some obvious differences among the three methods (Figure 4). Shadow detection of the NIR method works poorly on river region, with cases of over detection as show in Figure 4b and 4f. The Nagao's method and Brightness method show better shadow detection results than the NIR method on river region, and shadow do not confuse with water bodies by using the two methods (Figure 4c, 4d, 4h and 4i). We not only noted the NIR method also works poorly on darker materials with over detection, and we could see the obvious over detection on the fire scar region (Figure 4k).

Nagao's method and Brightness method also show a little over detection on the fire scar (Figure 4l and 4m). Darker materials are more easily confused with shadow. The results of Nagao's method and Brightness method are quite similar, and show better shadow detection than NIR method (Figure 4).
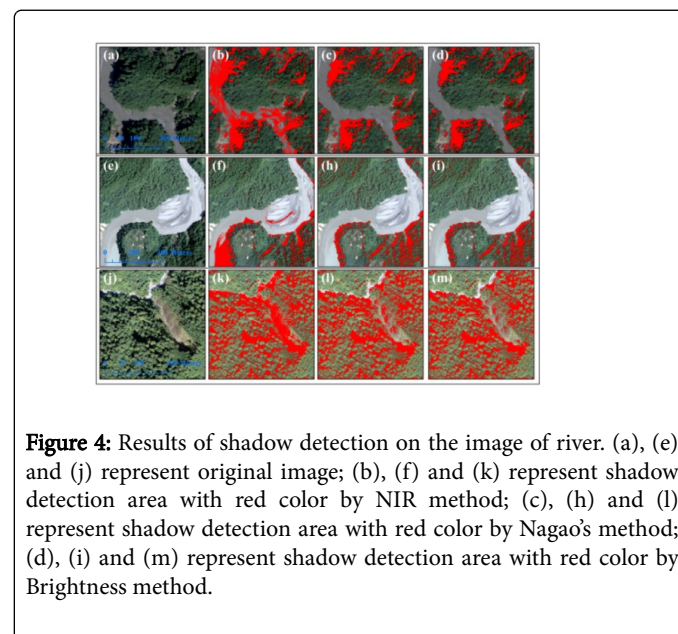
Figure 4: Results of shadow detection on the image of river. (a), (e) and (j) represent original image; (b), (f) and (k) represent shadow detection area with red color by NIR method; (c), (h) and (l) represent shadow detection area with red color by Nagao's method; (d), (i) and (m) represent shadow detection area with red color by Brightness method.

Comparison of shadow detection methods

In this study, we test three histogram thresholding methods, and the results indicate Brightness method and Nagao's method are significantly better than NIR method, however Brightness method and Nagao's method do not have significantly difference with each other.

Some papers indicate that NIR is sensitive to detect shadows, the NIR method could clearly distinguish shadowed regions [3,16]. However, shadow detection of the NIR method works poorly in the river region (Figure 4). Water bodies presented strong absorption in NIR, and show a lower reflectance in NIR. NIR often confuses water bodies with shadows due to the low reflectance of water [3].

The NIR method also works poorly on darker materials with over detection (Figure 4k), and it is also due to the lower reflectance of NIR of dark materials [3]. Some papers indicate panchromatic channels from high resolution satellite imagery (Ikonos, Quickbird) can clear classify shadow, but they also confuse water bodies or dark materials with shadows due to the lower reflectance of panchromatic channels [7,17].

NIR method was performed the lowest accuracy in the three methods. However, NIR method is delivered good results over 90% overall accuracy, and the accuracy is acceptable.

Nagao's method performs good shadow detection in this study (Average Overall Accuracy=94.45% (Table 2), and the results were consistent with previous studies [3,4,18]. Nagao's method show better discriminating from water bodies or dark materials than NIR method [3]. The Brightness method also performs good shadow detection (Average Overall Accuracy=94.75%) as Nagao's method in this study (Table 2). The results of Nagao's method and Brightness method are similar, since a similar formula for the two methods (e.g., 3 and 4). Those results indicate that used visible and NIR channels to generate a

new data space are better discriminate shadows from non-shadows [3,4,16].

In this study, we perform tree kinds of histogram thresholding methods, the performances of histogram thresholding methods depend on the selected data space [3,7]. The data space we used, Nagao et al. [4] modified intensity and Brightness are better than NIR channel to discriminate shadows from non-shadows, and the two methods are both not easily confused with shadow and water bodies. However, the Nagao's method and Brightness method still show some over detection on the darker materials (e.g., the fire scar in this study, see Figures 4l and 4m), and darker materials are more easily confused with shadow [7].

Histogram thresholding methods assumes that there is a clear separation between shadow and nonshadow histogram levels in a given data space to improve the separation of these two classes [3]. In our study, we found that most of cases presented shadow in the histogram of first mode. The shadow areas mainly contributed to the lower part of the histogram [7,18,19]. However, different data space produces different histogram shapes from bimodal to multi-modal distributions in this study. For example, the result of plot 4, we can notice that there are two peaks below the shadow optimal thresholds in the histogram of NIR (Figure 3g). Nagao's modified intensity and brightness were shown bimodal distribution in the histogram, first mode as the shadow threshold (Figure 3h and 3i). Therefore, a good data space and defining the optimum thresholding method will affect histogram thresholding result.

Conclusions

Three histogram thresholding methods were tested in this study, and the results indicate Brightness method and Nagao's method are significantly better than NIR method. NIR often confuses water bodies with shadows due to the low reflectance of water. The data space we used, Nagao's modified intensity and Brightness are better than NIR channel to discriminate shadows from non-shadows, and the two methods are both not easily confused with shadow and water bodies. In our study, we found that most of cases presented shadow in the histogram of first mode, and the first valley detection thresholding is a robust way to detect the shadow threshold of histogram. A good data space and defining the optimum thresholding method will affect histogram thresholding result.

In future, we can experiment other kinds of bands combinations to execute shadow detections. We suggested it can use hyperspectral data to detect shadows; also it can try to classify shadow and darker materials as method. We can utilize multi-combinations detection methods. Integrating 2-dimension spectral property-based shadow detection method and 3-dimension modeling shadow detection method to have a better performance.

Acknowledgements

References

1. Tsai VUD (2006) A comparative study on shadow compensation of color aerial images in invariant color models. IEEE Transactions on Geoscience and Remote Sensing 44: 1661-1671.

2. Tian J, Sun J, Tang Y (2009) Tricolor attenuation model for shadow detection. IEEE Transactions on Image Processing 18: 2355-2363.

3. Adeline KRM, Chen M, Briottet X, Pang SK, Paparoditis N (2013) Shadow detection in very high spatial resolution aerial images: A comparative study. ISPRS Journal of Photogrammetry and Remote Sensing 80: 21-38.

4. Nagao M, Matsutyama T, Ikeda Y (1979) Region extraction and shape analysis in aerial photos. Computer Graphics and Image Processing 10: 195-223.

5. Shu JSP, Freeman H (1990) Cloud shadow removal from aerial photographs. Pattern Recognition 23: 647-656.

6. Shettigara VK, Sumerling GM (1998) Height determination of extended objects using shadows in SPOT images. Photogrammetric Engineering & Remote Sensing 64: 35-44.

7. Dare PM (2005) Shadow analysis in high-resolution satellite imagery of urban areas. Photogrammetric Engineering & Remote Sensing 71: 169-177.

8. Chen Y, Wen D, Jing L, Shi P (2007) Shadow information recovery in urban areas from very high resolution satellite imagery. International Journal of Remote Sensing 28: 3249-3254.

9. Zhou W, Huang G, Troy A, Cadenasso ML (2009) Object-based land cover classification of shaded areas in high spatial resolution imagery of urban areas: A comparison study. Remote Sensing of Environment 113: 1769-1777.

10. Wu ST, Hsieh YT, Chen CT, Chen JC (2014) A Comparison of 4 Shadow Compensation Techniques for Land Cover Classification of Shaded Areas from High Radiometric Resolution Aerial Images. Canadian Journal of Remote Sensing 40: 315-326.

11. Rau JY, Chen NY, Chen LC (2002) True orthophoto generation of built-up areas using multi-view images. Photogrammetric Engineering & Remote Sensing 68: 581-588.

12. Li Y, Gong P, Sasagawa T (2005) Integrated shadow removal based on photogrammetry and image analysis. International Journal of Remote Sensing 26: 3911-3929.

13. Yao J, Zhang ZF (2006) Hierarchical shadow detection for color aerial images. Computer Vision and Image Understanding 102: 60-69.

14. Pateraki M, Baltsavias E (2003) Analysis and Performance of the Adaptive Multi-image matching Algorithm for Airborne Digital Sensor ADS40. In ASPRS Annual Conference, 5-9 May, Anchorage, AK, USA.

15. Blair DC (1979) Information Retrieval. In: Van Rijsbergen CJ (2nd edn.), Butterworths, London, J Am Soc Inf Sci 30: 374-375.

16. Fredembach C, Süsstrunk S (2010) Automatic and Accurate Shadow Detection from (Potentially) a Single Image using Near-Infrared Information. EPFL Technical Report 165527.

17. Yamazaki F, Liu W, Takasaki M (2009) Characteristics of shadow and removal of its effects for remote sensing imagery. In: Proc. International Geoscience and Remote Sensing Symposium, IGARSS, Cape Town, South, Africa, 12-17 July, pp: 426-429.

18. Wu J, Bauer ME (2013) Evaluating the effects of shadow detection on QuickBird image classification and spectroradiometric restoration. Remote Sensing 5: 4450-4469.

19. Yeh KS, Li MY, Wang YH (2010) Applying digital aerial images in natural hazards mitigation in Taiwan (In chinese). Journal of Photogrammetry and Remote Sensing 15: 123-140.